

Parallel Active Subspace Decomposition for Scalable and Efficient Tensor Robust Principal Component Analysis

Jonathan Q. Jiang and Michael K. Ng

Department of Mathematics, Hong Kong Baptist University

Abstract

Tensor robust principal component analysis (TRPCA) has received a substantial amount of attention in various fields. Most existing methods, normally relying on tensor nuclear norm minimization, need to pay an expensive computational cost due to multiple singular value decompositions (SVDs) at each iteration. To overcome the drawback, we propose a scalable and efficient method, named Parallel Active Subspace Decomposition (PASD), which divides the unfolding along each mode of the tensor into a columnwise orthonormal matrix (active subspace) and another small-size matrix in parallel. Such a transformation leads to a nonconvex optimization problem in which the scale of nuclear norm minimization is generally much smaller than that in the original problem. Furthermore, we introduce an alternating direction method of multipliers (ADMM) method to solve the reformulated problem and provide rigorous analyses for its convergence and suboptimality. Experimental results on synthetic and real-world data show that our algorithm is more accurate than the state-of-the-art approaches, and is orders of magnitude faster.

Keywords. Tensor robust principal component analysis, low-rank tensors, nuclear norm minimization, active subspace decomposition, low-rank matrix factorization

1 Introduction

The prevalence of multidimensional data, such as multichannel images and videos, in modern society, has revived our interest in the study for tensor decomposition, completion and recovery in last decade. Tensor, as higher-order generalization of vector and matrix, is able to take full advantage of the multilinear structure of the data and thus to provide better understanding and higher precision in signal processing [5], computer vision [18, 26], data mining [19, 24] and machine learning [14, 22].

Multidimensional data analysis traditionally relies on tensor decomposition [13], which normally takes two popular forms, CANDECOMP/PARAFAC (CP) decomposition [9] and Tucker decomposition [27]. Originated in the fields of psychometrics and chemometrics, these decompositions are now used in a wide range of application areas (see [13] for a comprehensive review). Owing to many factors, including the malfunctions in the acquisition process, loss of information, and expensive experiments, the multidimensional data is probably incomplete in many applications, which prevents both types of tensor decompositions from achieving satisfactory results. To address tensor data with missing values, two extended models called weighted Tucker [6] and weighted CP decomposition [1], have been recently proposed and successfully applied to EEG data analysis and image inpainting.

In reality, the intrinsic structures of the real data have been found to be actually low-rank, even if themselves may not be. Unlike matrices, the rank of a specific tensor is NP-hard to estimate in general [10] and

there exists no explicit expression for its tightest convex envelop so far. In the seminar work [18], the first convex approximation of tensor rank named tensor trace norm was given as a weighted combination of the trace norms of all matrices unfolded along each mode. Soon after, a large number of algorithms [7, 22, 23, 29] were proposed for the low-rank tensor completion (LRTC) problem, i.e., learning a low-rank tensor from partially observed data, on the basis of tensor trace norm minimization.

In this paper, we are particularly interested in another branch of the low-rank tensor recovery problem, namely Tensor Robust Principal Component Analysis (TRPCA). More precisely, we aim to split a noisy and fully observed tensor into a low-rank component that captures its underlying low-dimensional structure and a sparse component that contains the gross errors. This problem is essentially a tensor version of Robust Principal Component Analysis (RPCA) in matrix case [4]. Compared to the LRTC problem, investigations of the TRPCA problem are relatively limited and only can be found in a few papers [8, 12, 15, 25]. All the methods employed the tensor trace norm and tensor ℓ_1 norm to enforce the low-rankness and the sparsity of the two components respectively and depended on an alternating direction method of multipliers (ADMM) scheme, which suffered from a heavy computational burden due to the multiple singular value decompositions (SVDs) conducted in each iteration.

To address this issue, we propose an efficient and scalable method called Parallel Active Subspace Decomposition (PASD) in this paper. It is quite interesting and innovative from the following perspectives.

- Our PASD method simultaneously decomposes the unfolding along each mode of the tensor into a columnwise orthonormal matrix, e.g., active subspace [17], and another small-size matrix. The computational cost is significantly reduced, since the trace norms of the unfoldings are equivalently replaced by those of some smaller-size matrices.
- We introduce an effective and efficient ADMM algorithm to solve the nonconvex optimization problem, which seems particularly suitable for large-scale problems.
- We conduct rigorous analyses for the convergence and suboptimality of our algorithm.
- Experimental results show that our PASD method is much more accurate than the state-of-the-art approaches, especially when the Tucker rank is large, and is orders of magnitude faster.

We begin with a brief review of tensor basics and related works in Section 2. Section 3 gives our PASD model and its corresponding ADMM algorithm. In Section 4, we present the theoretical analyses for the convergence and suboptimality of our algorithm. Finally, we report experimental results in Section 5 and draw the conclusions in Section 6.

2 Notations and Preliminaries

Matrices are denoted by uppercase letters, e.g., X , and tensors by calligraphic letters, e.g., \mathcal{X} throughout the paper.

2.1 Tensor Basics

The order of a tensor is the number of dimensions, also known as ways or modes. Given a N -order tensor $\mathcal{X} \in \mathbb{R}^{I_1 \times \dots \times I_N}$, a fiber is a column vector defined by fixing every index of \mathcal{X} but one. The mode- n unfolding or matricization is the matrix denoted by $\mathcal{X}_{(n)} \in \mathbb{R}^{I_n \times \prod_{m \neq n} I_m}$ that is obtained by arranging the mode- n fibers to be the columns of the matrix. The mode- n product of a tensor $\mathcal{X} \in \mathbb{R}^{I_1 \times \dots \times I_N}$ with

a matrix $U \in \mathbb{R}^{J \times I_n}$ is defined as $(\mathcal{X} \times_n U)_{i_1 \dots i_{n-1} j_{n+1} \dots i_N} = \sum_{i_n=1}^{I_n} x_{i_1 \dots i_N} u_{j_{i_n}}$. The inner product of two tensors $\mathcal{X}, \mathcal{Y} \in \mathbb{R}^{I_1 \times \dots \times I_N}$ is defined as the sum of the product of their entries, i.e., $\langle \mathcal{X}, \mathcal{Y} \rangle = \sum_{i_1 \dots i_N} x_{i_1 \dots i_N} y_{i_1 \dots i_N}$, and the Frobenius norm of \mathcal{X} is defined as $\|\mathcal{X}\|_F = \sqrt{\langle \mathcal{X}, \mathcal{X} \rangle}$. The ℓ_1 norm and ℓ_∞ norm of a tensor \mathcal{X} are defined by its vectorization, i.e., $\|\mathcal{X}\|_1 = \|\text{vec}(\mathcal{X})\|_1$ and $\|\mathcal{X}\|_\infty = \|\text{vec}(\mathcal{X})\|_\infty$ respectively. The mode- n rank of \mathcal{X} is the column rank of $\mathcal{X}_{(n)}$. The set of N mode- n ranks (r_1, \dots, r_N) of a tensor \mathcal{X} is called its multilinear rank or Tucker rank.

2.2 Tensor Decompositions and Ranks

The CP decomposition [9] approximates a tensor as $\mathcal{X} \approx \sum_{i=1}^r \lambda_n \mathbf{a}_i^{(1)} \circ \mathbf{a}_i^{(2)} \circ \dots \circ \mathbf{a}_i^{(N)}$ where \circ stands for the outer product of two vectors, $\lambda_n \in \mathbb{R}$ and $\mathbf{a}_i^{(n)} \in \mathbb{R}^{I_n}$ for $i = 1, \dots, r$ and $n = 1, \dots, N$. The rank of \mathcal{X} is the smallest value of r such that the approximation holds with equality. The Tucker decomposition [27] is another factorization that approximates a tensor as $\mathcal{X} \approx \mathcal{C} \times_1 U_1 \times_2 U_2 \dots \times_N U_N$ where $\mathcal{C} \in \mathbb{R}^{r_1 \times \dots \times r_N}$ is the core tensor and $U_n \in \mathbb{R}^{I_n \times r_n}$, $n = 1, \dots, N$ are the factor matrices. The mode- n rank of \mathcal{X} is the column rank of $\mathcal{X}_{(n)}$. The set of N mode- n ranks (r_1, \dots, r_N) of a tensor \mathcal{X} is called its multilinear rank or Tucker rank.

2.3 Related work

Given a tensor data \mathcal{T} , the TRPCA problem can be mathematically represented by

$$\min_{\mathcal{X}, \mathcal{E}} \sum_{n=1}^N \lambda_n \|\mathcal{X}_{(n)}\|_* + \|\mathcal{E}\|_1, \quad \text{s.t.}, \mathcal{T} = \mathcal{X} + \mathcal{E}, \quad (2.1)$$

where \mathcal{X} and \mathcal{E} are the low-rank and sparse components, $\|\mathcal{X}_{(n)}\|_*$ denotes the trace norm of the unfolding $\mathcal{X}_{(n)}$, i.e., the sum of its singular values, and $\{\lambda_n\}$ are prespecified weights. Note that problem (2.1) is very difficult to solve because of the interdependent matrix trace norm terms.

The rank sparsity tensor decomposition (RSTD) algorithm [15] applies variable-splitting to both \mathcal{X} and \mathcal{E} , and utilizes a classic Block Coordinate Descent (BCD) approach to solve an unconstrained problem obtained by relaxing all the constraints as quadratic penalty terms. However, this method has many parameters to tune and does not have a iteration complexity guarantee. The Multi-linear Augmented Lagrange Multiplier (MALM) Method [25] is based on the ADMM algorithm and decomposes problem (2.1) into N independent standard RPCA instances. This relaxation makes the final solution hard to be optimal since consistency among the auxiliary variables is not considered. The Higher-order RPCA (HoRPCA) approach [8] is also an ADMM method that conducts variable-splitting on \mathcal{X} purely and reformulates problem (2.1) as

$$\begin{aligned} \min_{\mathcal{Z}_n, \mathcal{E}} \sum_{n=1}^N \lambda_n \|\mathcal{Z}_{n,(n)}\|_* + \|\mathcal{E}\|_1, \\ \text{s.t.}, \mathcal{T} = \mathcal{Z}_n + \mathcal{E}, \quad \forall n \in \mathbb{N} \end{aligned} \quad (2.2)$$

where $\{\mathcal{Z}_n\}$ are the auxiliary variables and \mathbb{N} is the index set $\{1, 2, \dots, N\}$. Note that equality among the \mathcal{Z}_n s is enforced implicitly by the constraints, so that additional auxiliary variables for \mathcal{E} as in [15, 25] are not required. Unfortunately, all the three approaches involve multiple SVDs of the unfoldings in each iteration, and thus are prone to suffer from expensive computational cost when the scale of the TRPCA problem is very large.

3 Our Method

In this section, we first introduce the PASD model for problem (2.2) and then propose an efficient ADMM iterative scheme to solve the new nonconvex optimization problem.

3.1 Parallel Active Subspace Decomposition

It is well-known that matrix factorization is one of the most useful tools in high-dimensional data analysis, on account of its high accuracy, scalability and flexibility to incorporating side information. Given a large-size matrix can be approximated by the product of two matrices with much smaller size. Inspired by the previous work [17], we decompose the unfoldings in problem (2.2) as

$$\mathcal{Z}_{n,(n)} = U_n V_n, \quad \text{s.t.}, U_n \in \text{St}(I_n, R_n), \quad \forall n \in \mathbb{N}$$

where $\text{St}(I_n, R_n)$ denotes the Stiefel manifold, i.e., the set of columnwise orthonormal matrices of size $I_n \times R_n$, and $r_n \leq R_n \ll I_n$ is a given upper bound on the mode- n rank of \mathcal{T} . The matrices $\{U_n\}$ are called active subspaces in [17], since the underlying principle behind such a decomposition is similar to the famous active set [20]. Due to the orthonormality of U_n s, we have that $\|\mathcal{Z}_{n,(n)}\|_* = \|U_n V_n\|_* = \|V_n\|_*$, $\forall n \in \mathbb{N}$, and problem (2.2) can be rewritten as

$$\begin{aligned} \min_{U_n, V_n, \mathcal{E}} \quad & \sum_{n=1}^N \lambda_n \|V_n\|_* + \|\mathcal{E}\|_1, \\ \text{s.t.}, \quad & \mathcal{T} = \text{fold}_n(U_n V_n) + \mathcal{E}, \quad U_n \in \text{St}(I_n, R_n), \quad \forall n \in \mathbb{N}, \end{aligned} \quad (3.1)$$

where $\text{fold}_n(A)$ returns the tensor \mathcal{A} such that $\mathcal{A}_{(n)} = A$. In (3.1), we carry out the active subspace decomposition along all modes in parallel and this is the main reason why we name our method. Note that there is a related work [28] which also makes use of parallel matrix factorization. But our study departs from it on the following two fronts. The problem considered in that work is obviously of different nature. That work mainly concentrated on the LRTC problem while ours focuses on the TRPCA problem. Besides, the standard low-rank matrix factorizations were used in that work, with no orthonormal constraint. More importantly, the trace norms are preserved in problem (3.1), which has been shown to be very helpful to the robustness of algorithms against outliers and non-Gaussian noise [3, 17, 21].

3.2 ADMM Algorithm

The ADMM method is very efficient for some convex or non-convex programming problems from various applications [2]. Therefore, we propose an ADMM algorithm to solve problem (3.1).

The partial augmented Lagrangian function for problem (3.1) is given by

$$\begin{aligned} \mathcal{L}_\mu(U_1 \cdots U_N, V_1 \cdots V_N, \mathcal{E}, \mathcal{Y}_1 \cdots \mathcal{Y}_N) \\ = \sum_{n=1}^N \left(\lambda_n \|V_n\|_* + \langle \mathcal{Y}_n, \mathcal{T} - \text{fold}_n(U_n V_n) - \mathcal{E} \rangle \right. \\ \left. + \frac{\mu}{2} \|\mathcal{T} - \text{fold}_n(U_n V_n) - \mathcal{E}\|_F^2 \right) + \|\mathcal{E}\|_1, \end{aligned} \quad (3.2)$$

where $\mathcal{Y}_n, \forall n \in \mathbb{N}$ are the tensors of Lagrange multipliers and μ is the penalty parameter. We give an iterative scheme to minimize \mathcal{L}_μ with respect to $\{U_n\}, \{V_n\}, \mathcal{E}$ successively.

By removing the terms irrelevant to U_n and adding some proper terms independent on U_n , problem (3.2) with respect to U_n can be simplified as

$$\min_{U_n} \|U_n V_n^k - G_n^k\|_F^2, \quad \text{s.t.}, U_n \in \text{St}(I_n, R_n), \quad (3.3)$$

where $G_n^k = \mathcal{T}_{(n)} - \mathcal{E}_{(n)}^k + \mathcal{Y}_{n,(n)}^k/\mu^k$. This is actually the well-known orthogonal procrustes problem [11]. Suppose the SVD of the matrix $G_n^k(V_n^k)^T$ is $G_n^k(V_n^k)^T = \widehat{U}_n^k \widehat{\Sigma}_n^k (\widehat{V}_n^k)^T$, and the optimal solution can be given by

$$U_n^{k+1} = \widehat{U}_n^k (\widehat{V}_n^k)^T. \quad (3.4)$$

By the similar way, problem (3.2) with respect to V_n can be reformulated as

$$\min_{V_n} \lambda_n \|V_n\|_* + \frac{\mu^k}{2} \|U_n^{k+1} V_n - G_n^k\|_F^2. \quad (3.5)$$

Considering that $U_n^{k+1} \in \text{St}(I_n, R_n)$, problem (3.4) is equivalent to

$$\min_{V_n} \lambda_n \|V_n\|_* + \frac{\mu^k}{2} \|V_n - (U_n^{k+1})^T G_n^k\|_F^2, \quad (3.6)$$

which has a closed-form solution

$$V_n^{k+1} = \text{SVT}_{\frac{\lambda_n}{\mu^k}} \left((U_n^{k+1})^T G_n^k \right). \quad (3.7)$$

The singular value thresholding (SVT) operator is defined by $\text{SVT}_\tau(X) = U \text{diag}(\max(\Sigma - \tau, 0)) V^T$ where the SVD of matrix X is $X = U \Sigma V^T$ and $\max(\cdot, \cdot)$ should be understood element-wise.

Fixing $\{U_n\}$ and $\{V_n\}$, we can update \mathcal{E} by solving

$$\min_{\mathcal{E}} \|\mathcal{E}\|_1 + \frac{\mu^k}{2} \sum_{n=1}^N \|\mathcal{E} - \mathcal{H}_n^k\|_F^2, \quad (3.8)$$

where $\mathcal{H}_n^k = \mathcal{T} - \text{fold}_n(U_n^{k+1} V_n^{k+1}) + \mathcal{Y}_n^k/\mu^k$. As indicated in [8], problem (3.7) has the following closed-form solution

$$\mathcal{E}^{k+1} = \text{prox}_{\frac{1}{\mu^k N}} \left(\frac{1}{N} \sum_{n=1}^N \mathcal{H}_n^k \right), \quad (3.9)$$

where $\text{prox}_\tau(\cdot)$ denotes the shrinkage operator, namely, $\text{prox}_\tau(x) = \text{sgn}(x) \max(|x| - \tau, 0)$.

Summarizing the above analysis, we obtain an ADMM algorithm for problem (3.1), as outlined in Algorithm 1. Note that the algorithm can be further accelerated by adaptively changing μ in each iteration (see line 7 in Algorithm 1).

4 Theoretical Analysis

In this section, we will provide complexity analysis for Algorithm 1 and present its several theoretical properties.

Algorithm 1 PASD: Solving (3.1) via ADMM

Input: \mathcal{T} , (R_1, \dots, R_n) , λ and ε .

Initialize: $U_n^0 = \text{eye}(I_n, R_n)$, $V_n^0 = 0$, $\mathcal{Y}_n^0 = 0$, $n = 1, \dots, N$, $\mathcal{E}^0 = 0$, $\mu^0 = 10^{-4}$, $\mu_{\max} = 10^{10}$ and $\rho = 1.1$.

- 1: **while** not converged **do**
- 2: Update U_n^{k+1} by (3.4).
- 3: Update V_n^{k+1} by (3.7).
- 4: Update \mathcal{E}^{k+1} by (3.9).
- 5: Compute $\mathcal{Z}_n^{k+1} = \text{fold}_n(U_n^{k+1}V_n^{k+1})$.
- 6: Update the multipliers \mathcal{Y}_n^{k+1} by
 $\mathcal{Y}_n^{k+1} = \mathcal{Y}_n^k + \mu^k(\mathcal{T} - \mathcal{Z}_n^{k+1} - \mathcal{E}^{k+1})$.
- 7: Update μ^{k+1} by $\mu^{k+1} = \min(\rho\mu^k, \mu_{\max})$.
- 8: Check the convergence condition,
 $\|\mathcal{T} - \mathcal{Z}_n^{k+1} - \mathcal{E}^{k+1}\|_\infty < \varepsilon, \forall n \in \mathbb{N}$.
- 9: **end while**

Output: $\mathcal{X} = \frac{1}{\sum_{n=1}^N \alpha_n} \sum_{n=1}^N \alpha_n \mathcal{Z}_n$.

4.1 Complexity Analysis

The running time of Algorithm 1 is dominated by conducting SVD on much smaller matrices of sizes $I_n \times R_n$ and $R_n \times \prod_{m \neq n} I_m$, $n \in \mathbb{N}$. The time complexity of performing SVD in (3.4) and in (3.7) are $O(R_n^2 I_n)$ and $O(R_n^2 \prod_{m \neq n} I_m)$, respectively. The time complexity of some matrix multiplications is $O(R_n \prod_n I_n)$. Therefore, the total time complexity of Algorithm 1 is $O(T \sum_n (R_n^2 I_n + R_n^2 \prod_{m \neq n} I_m + R_n \prod_n I_n))$ where T is the number of iterations. Without loss of generality, we assume that the time complexity of Algorithm 1 in each iteration is only $O(NRI^N)$ provided that the sizes of the input tensors are $I_1 = \dots = I_n = I$ and the given ranks are $R_1 = \dots = R_n = R$ ($R \ll I$). Recall that the complexities of most existing approaches, e.g. MALM [25], SNN [12] and HoRPCA [8], in each iteration are all $O(NI^{N+1})$. Thus, our PASD method is much more efficient, as shown in the experiments later.

4.2 Convergence Analysis

Next, we check the convergence of our proposed algorithm. In fact, Algorithm 1 can stop within a finite number of iterations, as shown in the following theorem.

Theorem 4.1 *Let $(\{U_1^k \dots U_N^k\}, \{V_1^k \dots V_N^k\}, \mathcal{E}^k)$ be a sequence generated by Algorithm 1, then we have that*

(I) *The sequences $\{V_n^k\}$, $\{U_n^k V_n^k\}$, $\forall n \in \mathbb{N}$ and $\{\mathcal{E}^k\}$ are Cauchy sequences respectively.*

(II) *$(U_n^k, V_n^k, \mathcal{E}^k)$ is a feasible solution to problem (3.1) in a sense that*

$$\lim_{k \rightarrow \infty} \|\mathcal{T} - \text{fold}_n(U_n^k V_n^k) - \mathcal{E}^k\|_\infty < \varepsilon, \forall n \in \mathbb{N}.$$

The proof of Theorem 4.1 is quite similar to those in [16, 17]. We first introduce two additional groups of auxiliary Lagrangian multipliers,

$$\hat{\mathcal{Y}}_n^{k+1} = \mathcal{Y}_n^k + \mu^k(\mathcal{T} - \text{fold}_n(U_n^{k+1}V_n^{k+1}) - \mathcal{E}^k), \quad (4.1)$$

$$\bar{\mathcal{Y}}_n^{k+1} = \mathcal{Y}_n^k + \mu^k(\mathcal{T} - \text{fold}_n(U_n^{k+1}V_n^k) - \mathcal{E}^k), \quad (4.2)$$

for $n \in \mathbb{N}$ and study the boundedness of them as well as some variables in Algorithm 1, which are summarized in the following lemma.

Lemma 4.2 *The sequences $\{\mathcal{Y}_n^k\}$, $\{\hat{\mathcal{Y}}_n^k\}$, $\{\bar{\mathcal{Y}}_n^k\}$, $\{\mathcal{E}^k\}$, $\{V_n^k\}$, and $\{U_n^k V_n^k\}$, $\forall n \in \mathbb{N}$ are all bounded.*

We can then use this lemma to prove Theorem 4.1. The detailed proof is given in Appendix A and B.

4.3 Suboptimality Analysis

In this subsection, we attempt to show that it is possible to prove the local optimality of the solution produced by Algorithm 1. In other words, we want to investigate the gap between the true minimum and the minimal value of the objective function achieved by our proposed algorithm.

Let k^* be the number of iterations when Algorithm 1 stops, and $U_n^* = U_n^{k^*+1}$, $V_n^* = V_n^{k^*+1}$, and $\mathcal{E}^* = \mathcal{E}^{k^*+1}$ respectively. Besides, \mathcal{Y}_n^* and $\hat{\mathcal{Y}}_n^*$ denote the Lagrange multipliers $\mathcal{Y}_n^{k^*+1}$ and $\hat{\mathcal{Y}}_n^{k^*+1}$ corresponding to $(\{U_n^*\}, \{V_n^*\}, \mathcal{E}^*)$. Then we have the following lemma whose proof can be found in Appendix C.

Lemma 4.3 *Given the solution $(\{U_n^*\}, \{V_n^*\}, \mathcal{E}^*)$ generated by Algorithm 1, the following conclusion holds*

$$\begin{aligned} \sum_{n=1}^N \lambda_n \|V_n\|_* + \|\mathcal{E}\|_1 &\geq \sum_{n=1}^N \lambda_n \|V_n^*\|_* + \|\mathcal{E}^*\|_1 \\ &+ \sum_{n=1}^N \langle \mathcal{Y}_n^* - \hat{\mathcal{Y}}_n^*, \mathcal{E} - \mathcal{E}^* \rangle - \sum_{n=1}^N \lambda_n I_n \prod_{m \neq n} I_m \mathcal{E}, \end{aligned} \quad (4.3)$$

for any feasible solution $(\{U_n\}, \{V_n\}, \mathcal{E})$ to problem (3.1).

To reach the global optimality of problem (3.1), we are required to show that the term $\sum_{n=1}^N \langle \mathcal{Y}_n^* - \hat{\mathcal{Y}}_n^*, \mathcal{E} - \mathcal{E}^* \rangle$ almost surely vanishes. According to the proofs of Theorem 4.1 and Lemma 4.3 (see the Supplementary Materials), we can conclude that

$$\begin{aligned} \left\| \sum_{n=1}^N (\mathcal{Y}_n^* - \hat{\mathcal{Y}}_n^*) \right\|_\infty &\leq \left\| \sum_{n=1}^N \mathcal{Y}_n^* \right\|_\infty + \sum_{n=1}^N \|\hat{\mathcal{Y}}_n^*\|_\infty \\ &\leq 1 + \sum_{n=1}^N \lambda_n \end{aligned} \quad (4.4)$$

which means that $\sum_{n=1}^N (\mathcal{Y}_n^* - \hat{\mathcal{Y}}_n^*)$ is bounded. By setting the parameter ρ to be relatively small (e.g., $\rho = 1.1$ as suggested in [17]), $\sum_{n=1}^N (\mathcal{Y}_n^* - \hat{\mathcal{Y}}_n^*)$ can be sufficiently small. Let $\epsilon = \left\| \sum_{n=1}^N (\mathcal{Y}_n^* - \hat{\mathcal{Y}}_n^*) \right\|_\infty$, then we have the following theorems.

Theorem 4.4 Let f^g be the globally optimal objective function value of (3.1), and f^* be the objective function value of (3.1) generated by Algorithm 1. We have that

$$f^* \leq f^g + c\epsilon + \sum_{n=1}^N \lambda_n I_n \prod_{m \neq n} I_m \epsilon \quad (4.5)$$

where c is a constant defined by

$$c = \frac{1}{\mu^0 N^2} \sum_{n=1}^N I_n \prod_{m \neq n} I_m \left(\frac{\rho(1+\rho)}{\rho-1} + \frac{1}{2\rho^{k^*}} \right) + \|\mathcal{T}\|_1$$

Theorem 4.5 Suppose $(\mathcal{X}^o, \mathcal{E}^o)$ is an optimal solution to problem (2.1), the Tucker rank of \mathcal{X}^o is (r_1, \dots, r_N) , and $f^o = \sum_{n=1}^N \alpha_n \|\mathcal{X}_{(n)}^o\|_* + \lambda \|\mathcal{E}^o\|_1$. Let f^* be the objective function value of (3.1) returned by Algorithm 1, then we have

$$\begin{aligned} f^o \leq f^* \leq f^o + c\epsilon + \sum_{n=1}^N \lambda_n I_n \prod_{m \neq n} I_m \epsilon \\ + \sum_{n=1}^N \lambda_n \left(\sqrt{I_n \prod_{m \neq n} I_m} - 1 \right) \sigma_{(n)}^{R_n+1} \max(r_n - R_n, 0), \end{aligned} \quad (4.6)$$

where $\sigma_{(n)}^i$ is the i th largest singular value of $\mathcal{X}_{(n)}^o$.

The proofs of Theorem 4.4 and 4.5 can be found in Appendix D and E. These two theorems reduce to their counterparts, Theorem 3.1 and 3.2 in [17], provided that the tensors are two-dimensional matrices.

5 Experiments and Discussions

In this section, we systematically evaluate the effectiveness and efficiency of our PASD method on synthetic and real-world data. All the experiments are performed with MATLAB 8.1 on an Intel Xeon E5-2620 workstation with 2.0-GHz CPU and 24-GB memory.

5.1 Synthetic Tensor Recovery

We generate a low-rank tensor $\mathcal{T}_0 \in \mathbb{R}^{I_1 \times \dots \times I_N}$, which is used as ground truth, by the Tucker decomposition model. As described in [], we draw the entries of the core tensor $\mathcal{C} \in \mathbb{R}^{r_1 \times \dots \times r_N}$ from the standard normal distribution $\mathcal{N}(0, 1)$ and multiply each mode of the core tensor by an columnwise orthonormal factor matrix $U_n \in \mathbb{R}^{I_n \times r_n}$ drawn from the Haar measure. All generated tensors were verified to have the desired Tucker rank. A random fraction ρ_n of the tensor elements were corrupted by additive i.i.d. noise from the uniform distribution $\mathcal{U}[-1, 1]$.

We recover the low-rank tensor by our PASD algorithm and compare it with two state-of-the-art approaches, MALM [25] and SNN [12]. We also conduct RPCA [4] on the unfoldings along all the modes and report the best result. Without loss of generality, we set the size of tensor to be $100 \times 100 \times 100$ and $50 \times 50 \times 50 \times 50$ respectively and fix the Tucker rank to be $r_n = 10, \forall n \in \mathbb{N}$. We set $\epsilon = 10^{-5}$ and

Table 1: RSE and running time (seconds) comparison on synthetic tensor data.

(a) Tensor size: $100 \times 100 \times 100$								
	RPCA		MALM		SNN		PASD	
ρ_n	RSE	Time	RSE	Time	RSE	Time	RSE	Time
5%	1.87e-7	35.50	1.80e-7	164.26	1.28e-7	171.21	1.12e-7	54.89
10%	3.92e-7	54.66	4.69e-5	169.97	9.91e-7	185.48	1.28e-7	55.95
20%	8.08e-4	65.78	1.98e-3	189.67	1.22e-6	207.74	1.44e-7	57.65
(a) Tensor size: $50 \times 50 \times 50 \times 50$								
	RPCA		MALM		SNN		PASD	
ρ_n	RSE	Time	RSE	Time	RSE	Time	RSE	Time
5%	4.57e-3	300.34	3.50e-3	1191.80	3.30e-3	1750.07	2.99e-3	469.46
10%	1.20e-2	453.26	7.74e-3	1777.02	9.02e-3	1782.93	8.33e-3	483.37
20%	9.63e-1	611.13	9.39e-1	2344.38	4.72e-2	2286.70	4.27e-2	544.28

maxiter = 1000 for all the algorithms. The parameter λ for RPCA and MALM are set to be the default values. For SNN and PASD, the parameters λ_n are set as $\frac{\sqrt{\max(I_n, \prod_{j \neq i} I_j)}}{N}$. The upper bound of Tucker ranks are chosen as $R_n = R = \lfloor 1.2r \rfloor, \forall n \in \mathbb{N}$ for PASD. The relative square error (RSE) of the recovered tensor \mathcal{X} is measured by $\text{RSE} = \|\mathcal{X} - \mathcal{T}_0\|_F / \|\mathcal{T}_0\|_F$.

The average results (RSE and computational time) of ten independent runs are summarized in Table 1, where ρ_n is set to 5%, 10% or 20%. We can see clearly that the PASD algorithm always outperforms the other approaches in terms of RSE and efficiency in all the cases. In particular, it can yield much more accurate solutions using less time for synthetic tensors of size $50 \times 50 \times 50 \times 50$ which is much more difficult to be recovered due to the relatively large ratio of the Tucker rank and tensor size. The empirical performance of all these methods can be measured using phase transition plots, which use grayscale colors to depict how likely a certain kind of low-rank tensors can be recovered by those algorithms for a range of different ranks from errors of varying sparsity. If the relative error $\text{RSE} \leq 10^{-3}$, we declare the trial to be successful. Fig. 1 shows the phase transition plots of all algorithms on the third-order tensors of size $100 \times 100 \times 100$, where the x -axis corresponds to the Tucker rank $r_n, \forall n \in \mathbb{N}$ changing from 2 to 50 with increment 2, and the y -axis denotes ρ_n varying from 2% to 50% with increment 2%. For each setting, ten independent trials were run.

Next, we check the running time of all the methods on the 3-order tensors with varying sizes. As shown in Figure 2, the running time of PASD increases much more slowly than those of the other approaches, which indicates that our PASD method is quite suitable for large-scale applications.

5.2 MRI Image Restoration

In this experiment, we compare our PASD method with other approaches on the brain MRI image data, which is of size $181 \times 217 \times 181$ and is approximately low-rank [18]. We randomly choose ρ_n percentage of pixels for each image to be corrupted by random values in $[0, 255]$, where ρ_n varies from 5% to 30%. We employ the Peak Signal to Noise Ratio (PSNR) to measure the difference between original image and the images recovered by various methods. For a specific ρ_n , the experiment is repeated 10 times and the average results are reported in Table 2, where the parameters for all the methods are set as in the synthetic experiments and the upper bound of Tucker ranks are chosen as $R_n = 40, \forall n \in \mathbb{N}$ for PASD.

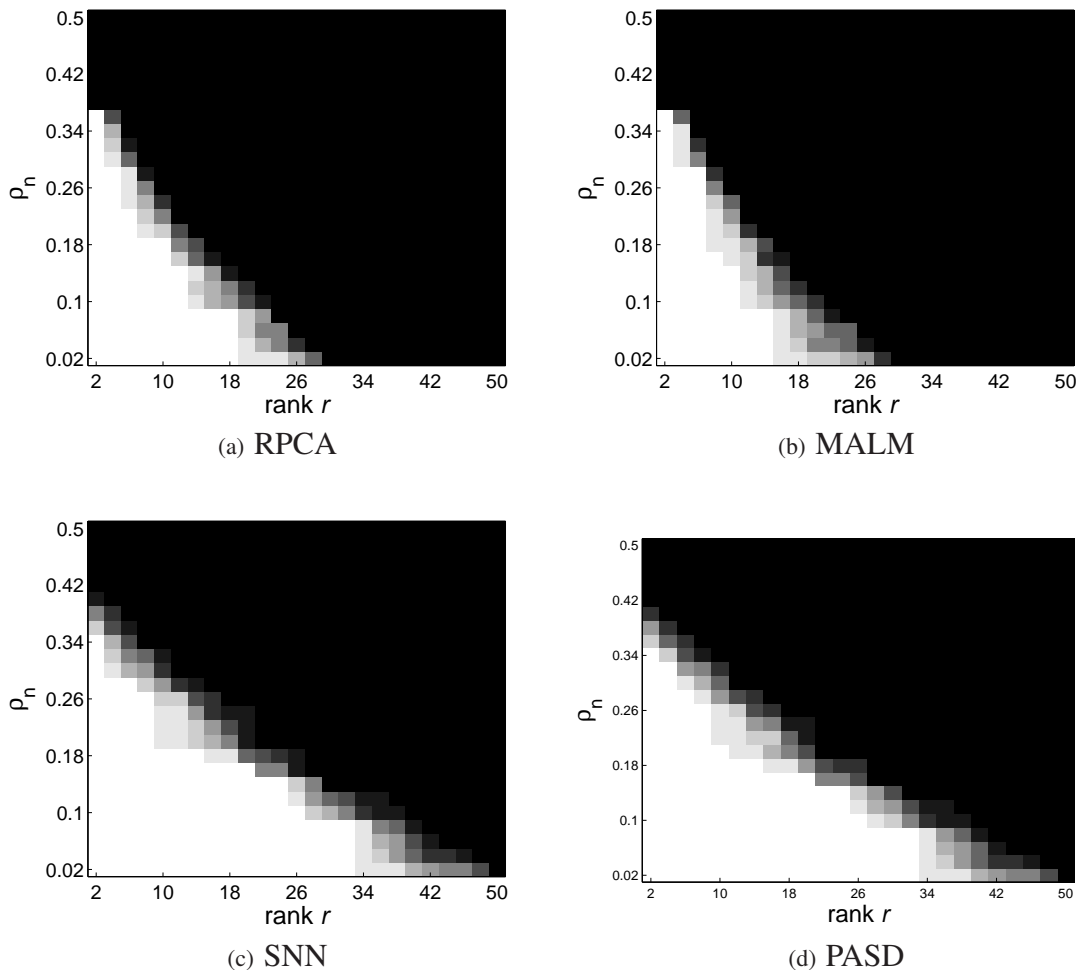


Figure 1: Phase transition plots on the third-order tensors. White region: 100% success and black region: 0% success in all experiments.

6 Conclusions

In this paper, we propose a scalable and efficient method for the TRPCA problem. Considering that the heavy computational cost in the existing approaches are all stemming from the multiple SVDs conducted in each iteration, we split the unfoldings along each mode of the tensor into a columnwise orthonormal matrix (active subspace) and another small-size matrix. Such a transformation seems somewhat absurd, since it reformulate a convex optimization problem as a nonconvex one that is much more difficult to solve in general. But this reformulation indeed allows us to replace the trace norm minimizations with large size by those involved some smaller-size matrices, and thus to reduce the computational complexity from $O(NI^{N+1})$ to $O(NRI^N)$ in each iteration. Therefore, our algorithm can scale pretty well to large-scale applications. The experiments show that our algorithm outperforms the state-of-the-art approaches in terms of both accuracy and efficiency. We expect that our PASD method can shed light on the development of new scalable algorithms for the problem of low-rank tensor recovery.

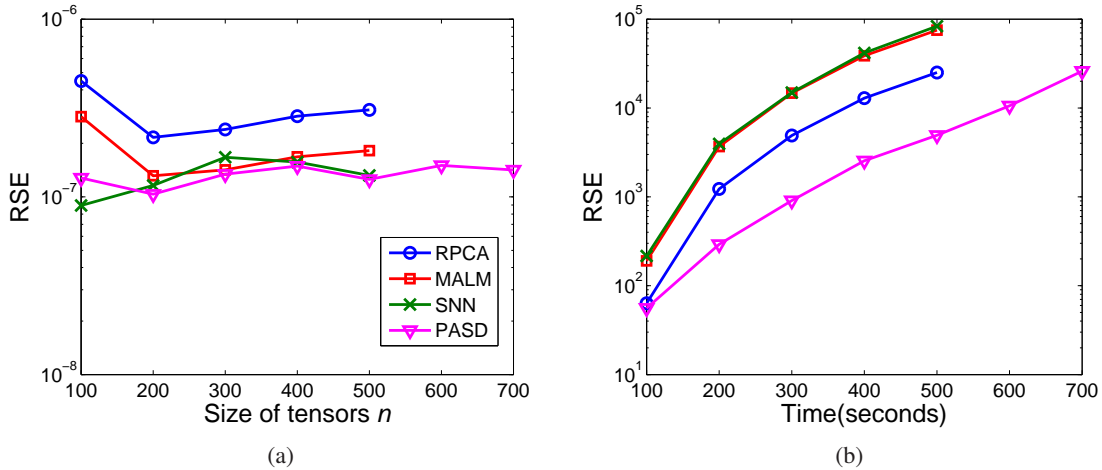


Figure 2: Comparison of all these methods in terms of RSE and computational time (in logarithmic scale) on the third-order tensors by varying given tensor sizes.

Table 2: Average PSNR and running time (seconds) comparison on brain MRI data.

ρ_n	RPCA		MALM		SNN		PASD	
	PSNR	Time	PSNR	Time	PSNR	Time	PSNR	Time
0.05	47.96	529.91	48.07	1282.10	56.23	1482.00	56.22	324.97
0.10	46.89	517.95	47.02	1386.86	56.05	1281.08	56.02	311.23
0.15	45.07	392.70	45.27	1077.11	55.64	1069.74	55.58	270.69
0.20	42.62	399.76	42.97	977.63	54.76	1052.47	54.70	267.53
0.25	39.73	285.75	40.02	828.34	52.39	1047.31	52.36	271.87
0.30	36.59	289.81	36.81	837.23	48.69	899.38	48.74	264.41

References

- [1] Evrim Acar, Daniel M. Dunlavy, Tamara G. Kolda, and Morten Mørup. Scalable tensor factorizations with missing data. In *SIAM International Conference on Data Mining*, pages 701–712, 2010.
- [2] Stephen Boyd, Neal Parikh, Eric Chu, Borja Peleato, and Jonathan Eckstein. Distributed optimization and statistical learning via the alternating direction method of multipliers. *Foundations & Trends in Machine Learning*, 3(1):1–122, 2011.
- [3] Ricardo Cabral, Fernando De La Torre, João P. Costeira, and Alexandre Bernardino. Unifying nuclear norm and bilinear factorization approaches for low-rank matrix decomposition. In *IEEE International Conference on Computer Vision*, pages 2488–2495, 2013.
- [4] Candès, Emmanuel J. S, Xiaodong Li, Yi Ma, and John Wright. Robust principal component analysis? *Journal of the ACM*, 58(3):1–73, 2011.
- [5] Andrzej Cichocki, Danilo Mandic, Lieven De Lathauwer, and Guoxu Zhou. Tensor decompositions for signal processing applications: From two-way to multiway component analysis. *IEEE Signal Processing Magazine*, 32(2):145–163, 2014.

- [6] Marko Filipović and Ante Jukić. Tucker factorization with missing data with application to low- n -rank tensor completion. *Multidimensional Systems & Signal Processing*, 26(3):1–16, 2013.
- [7] Silvia Gandy, Benjamin Recht, and Isao Yamada. Tensor completion and low- n -rank tensor recovery via convex optimization. *Inverse Problems*, 27(2):25010–25028(19), 2011.
- [8] Donald Goldfarb and Zhiwei Qin. Robust low-rank tensor recovery: Models and algorithms. *SIAM Journal on Matrix Analysis & Applications*, 35(1):225–253, 2013.
- [9] Richard A. Harshman. Foundations of the parafac procedure: Model and conditions for an “explanatory” multi-mode factor analysis. In *UCLA Working Papers*, 1969.
- [10] Johan Håstad. Tensor rank is np-complete. *Journal of Algorithms*, 11(4):451–460, 2006.
- [11] Nick Higham. *Matrix procrustes problems*. 1995.
- [12] Bo Huang, Cun Mu, Donald Goldfarb, and John Wright. Provable models for robust low-rank tensor completion. *Pacific Journal of Optimization*, 11(2):339–364, 2015.
- [13] Tamara G. Kolda and Brett W. Bader. Tensor decompositions and applications. *SIAM Review*, 66(4):294–310, 2005.
- [14] Xuelong Li, Stephen Lin, Shuicheng Yan, and Dong Xu. Discriminant locally linear embedding with high-order tensor data. *IEEE Transactions on Systems Man & Cybernetics Part B Cybernetics*, 38(2):342–352, 2008.
- [15] Yin Li, Junchi Yan, Yue Zhou, and Jie Yang. Optimum subspace learning and error correction for tensors. In *European Conference on Computer Vision*, pages 790–803, 2010.
- [16] Zhouchen Lin, Minming Chen, and Yi Ma. The augmented lagrange multiplier method for exact recovery of corrupted low-rank matrices. Technical report, Univ. Illinois, Urbana-Champaign, 2009.
- [17] G. Liu and S. Yan. Active subspace: toward scalable low-rank learning. *Neural Computation*, 24(12):3371–3394, 2012.
- [18] Ji Liu, Przemyslaw Musialski, Peter Wonka, and Jieping Ye. Tensor completion for estimating missing values in visual data. *IEEE Transactions on Pattern Analysis & Machine Intelligence*, 35(1):208–220, 2013.
- [19] Morten Mørup. Applications of tensor (multiway array) factorizations and decompositions in data mining. *Wiley Interdisciplinary Reviews Data Mining & Knowledge Discovery*, 1(1):24–40, 2011.
- [20] By Jorge Nocedal and Stephen J Wright. *Numerical optimization*. Springer-Verlag, 2006.
- [21] M. Okutomi, Shuicheng Yan, S. Sugimoto, Guangcan Liu, and Yinqiang Zheng. Practical low-rank matrix approximation under robust ℓ_1 -norm. In *IEEE Conference on Computer Vision and Pattern Recognition*, pages 1410–1417, 2012.
- [22] Marco Signoretto, Quoc Tran Dinh, Lieven De Lathauwer, and Johan A. K. Suykens. Learning with tensors: a framework based on convex optimization and spectral regularization. *Machine Learning*, 94(3):303–351, 2014.

- [23] Marco Signoretto, Lieven De Lathauwer, and Johan A K Suykens. Nuclear norms for tensors and their use for convex multilinear estimation. 2010.
- [24] Jimeng Sun, Spiros Papadimitriou, Ching Yung Lin, Nan Cao, Shixia Liu, and Weihong Qian. Multivis: Content-based social network exploration through multi-way visual analysis. In *SIAM International Conference on Data Mining*, pages 1064–1075, 2009.
- [25] Huachun Tan, Bin Cheng, Jianshuai Feng, Guangdong Feng, Wuhong Wang, and Yu Jin Zhang. Low-rank tensor recovery based on multi-linear augmented lagrange multiplier method. *Neurocomputing*, 119(16):144–152, 2013.
- [26] Dacheng Tao, Xuelong Li, Xindong Wu, and Stephen J. Maybank. General tensor discriminant analysis and gabor features for gait recognition. *IEEE Transactions on Pattern Analysis & Machine Intelligence*, 29(10):1700–15, 2007.
- [27] Ledyard R Tucker. Some mathematical notes on three-mode factor analysis. *Psychometrika*, 31(3):279–311, 1966.
- [28] Yangyang Xu, Ruru Hao, Wotao Yin, and Zhixun Su. Parallel matrix factorization for low-rank tensor completion. *Inverse Problems & Imaging*, 9(2), 2015.
- [29] Lei Yang, Zheng Hai Huang, and Xianjun Shi. A fixed point iterative method for low n-rank tensor pursuit. *IEEE Transactions on Signal Processing*, 61(11):2952–2962, 2013.

A Proof of Lemma 4.2

To prove the boundedness of the sequences, we first introduce the following lemma.

Lemma A.1 [16] *Let \mathcal{H} be a real Hilbert space endowed with an inner product $\langle \cdot, \cdot \rangle$ and a corresponding norm $\| \cdot \|$, and $\mathbf{y} \in \partial \| \mathbf{x} \|$, where $\partial \| \cdot \|$ denotes the subgradient. Then $\| \mathbf{y} \| = 1$ if $\mathbf{x} \neq \mathbf{0}$, and $\| \mathbf{y} \| \leq 1$ if $\mathbf{x} = \mathbf{0}$, where $\| \cdot \|$ is the dual norm of the norm $\| \cdot \|$.*

As mentioned in the paper, we propose an ADMM scheme to circularly minimize \mathcal{L}_μ with respect to $\{U_n\}$, $\{V_n\}$, \mathcal{E} and update \mathcal{Y}_n as follow.

$$\min_{\{U_n\}} \mathcal{L}_{\mu^k}(U_1 \cdots U_N, V_1^k \cdots V_N^k, \mathcal{E}^k, \mathcal{Y}_1^k \cdots \mathcal{Y}_N^k) \quad (\text{A.1})$$

$$\text{s.t., } U_n \in \text{St}(I_n, R_n),$$

$$\min_{\{V_n\}} \mathcal{L}_{\mu^k}(U_1^{k+1} \cdots U_N^{k+1}, V_1 \cdots V_N, \mathcal{E}^k, \mathcal{Y}_1^k \cdots \mathcal{Y}_N^k), \quad (\text{A.2})$$

$$\min_{\mathcal{E}} \mathcal{L}_{\mu^k}(U_1^{k+1} \cdots U_N^{k+1}, V_1^{k+1} \cdots V_N^{k+1}, \mathcal{E}, \mathcal{Y}_1^k \cdots \mathcal{Y}_N^k), \quad (\text{A.3})$$

$$\mathcal{Y}_n^{k+1} = \mathcal{Y}_n^k + \mu^k (\mathcal{T} - \text{fold}_n(U_n^{k+1} V_n^{k+1}) - \mathcal{E}^{k+1}). \quad (\text{A.4})$$

Proof For convenience, we denote $\mathfrak{U}^k = (U_1^k, \dots, U_N^k)$, $\mathfrak{V}^k = (V_1^k, \dots, V_N^k)$ and $\mathfrak{Y}^k = (\mathcal{Y}_1^k, \dots, \mathcal{Y}_N^k)$. The first order optimal condition of problem (A.3) with respect to \mathcal{E}^{k+1} is

$$\mathbf{0} \in \partial_{\mathcal{E}^{k+1}} \mathcal{L}_{\mu^k}(\mathfrak{U}^{k+1}, \mathfrak{V}^{k+1}, \mathcal{E}^{k+1}, \mathfrak{Y}^k),$$

i.e.,

$$\sum_{n=1}^N \left(\mathcal{Y}_n^k + \mu^k (\mathcal{T} - \text{fold}_n(U_n^{k+1} V_n^{k+1}) - \mathcal{E}^{k+1}) \right) \in \partial \|\mathcal{E}^{k+1}\|_1,$$

which implies that

$$\sum_{n=1}^N \mathcal{Y}_n^{k+1} \in \partial \|\mathcal{E}^{k+1}\|_1.$$

By Lemma A.1, we have

$$\left\| \sum_{n=1}^N \mathcal{Y}_n^{k+1} \right\|_\infty \leq 1. \quad (\text{A.5})$$

Hence, the sequence $\{\mathcal{Y}_n^k\}, \forall n \in \mathbb{N}$ are all bounded.

The optimality of U_n^{k+1} directly leads us to that

$$\begin{aligned} \|\bar{\mathcal{Y}}_n^{k+1}\|_F &= \|\mathcal{Y}_n^k + \mu^k (\mathcal{T} - \text{fold}_n(U_n^{k+1} V_n^k) - \mathcal{E}^k)\|_F \\ &\leq \|\mathcal{Y}_n^k + \mu^k (\mathcal{T} - \text{fold}_n(U_n^k V_n^k) - \mathcal{E}^k)\|_F \\ &= \|(1 + \rho)\mathcal{Y}_n^k - \rho\mathcal{Y}_n^{k-1}\|_F \end{aligned} \quad (\text{A.6})$$

So $\{\bar{\mathcal{Y}}_n^k\}, \forall n \in \mathbb{N}$ are bounded due to the boundedness of $\{\mathcal{Y}_n^k\}, \forall n \in \mathbb{N}$.

The first-order optimal condition for problem (A.2) with respect to V_n^{k+1} is given by

$$\mathbf{0} \in \partial_{V_n^{k+1}} \mathcal{L}_{\mu^k}(\mathfrak{U}^{k+1}, \mathfrak{V}^{k+1}, \mathcal{E}^k, \mathfrak{Y}^k),$$

which gives that

$$(U_n^{k+1})^T \hat{\mathcal{Y}}_{n,(n)}^{k+1} \in \lambda_n \partial \|V_n^{k+1}\|_*.$$

By Lemma A.1, we know that

$$\|(U_n^{k+1})^T \hat{\mathcal{Y}}_{n,(n)}^{k+1}\| \leq \lambda_n, \quad (\text{A.7})$$

and thus $\{(U_n^{k+1})^T \hat{\mathcal{Y}}_{n,(n)}^{k+1}\}, \forall n \in \mathbb{N}$ are bounded. Let $(U_n^{k+1})^\perp$ denote the orthogonal complement of U_n^{k+1} , and we can easily check that

$$\left((U_n^{k+1})^\perp \right)^T \hat{\mathcal{Y}}_{n,(n)}^{k+1} = \left((U_n^{k+1})^\perp \right)^T \bar{\mathcal{Y}}_{n,(n)}^{k+1}$$

which immediately implies

$$\left\| \left((U_n^{k+1})^\perp \right)^T \hat{\mathcal{Y}}_{n,(n)}^{k+1} \right\| = \left\| \left((U_n^{k+1})^\perp \right)^T \bar{\mathcal{Y}}_{n,(n)}^{k+1} \right\| \leq \|\bar{\mathcal{Y}}_{n,(n)}^{k+1}\|. \quad (\text{A.8})$$

Therefore, $\left\{ \left((U_n^{k+1})^\perp \right)^T \hat{\mathcal{Y}}_{n,(n)}^{k+1} \right\}, \forall n \in \mathbb{N}$ are bounded. According to these two facts, $\{\hat{\mathcal{Y}}_n^k\}, \forall n \in \mathbb{N}$ are bounded as well.

By the iteration procedure of Algorithm 1, we have

$$\begin{aligned} \mathcal{L}_{\mu^k}(\mathfrak{U}^{k+1}, \mathfrak{V}^{k+1}, \mathcal{E}^{k+1}, \mathfrak{Y}^k) &\leq \mathcal{L}_{\mu^k}(\mathfrak{U}^{k+1}, \mathfrak{V}^{k+1}, \mathcal{E}^k, \mathfrak{Y}^k) \\ &\leq \mathcal{L}_{\mu^k}(\mathfrak{U}^{k+1}, \mathfrak{V}^k, \mathcal{E}^k, \mathfrak{Y}^k) \\ &\leq \mathcal{L}_{\mu^k}(\mathfrak{U}^k, \mathfrak{V}^k, \mathcal{E}^k, \mathfrak{Y}^k) \\ &= \mathcal{L}_{\mu^{k-1}}(\mathfrak{U}^k, \mathfrak{V}^k, \mathcal{E}^k, \mathfrak{Y}^{k-1}) + \sum_{n=1}^N \frac{\mu^{k-1} + \mu^k}{2(\mu^{k-1})^2} \|\mathcal{Y}_n^k - \mathcal{Y}_n^{k-1}\|_F^2. \end{aligned} \quad (\text{A.9})$$

Note that $\mu^k = \rho\mu^{k-1}$ and we have

$$\sum_{k=1}^{\infty} \frac{\mu^{k-1} + \mu^k}{2(\mu^{k-1})^2} = \frac{\rho(\rho+1)}{2\mu^0(\rho-1)} < \infty.$$

Hence, $\{\mathcal{L}_{\mu^k}(\mathcal{U}^k, \mathfrak{Y}^k, \mathcal{E}^k, \mathfrak{Y}^{k-1})\}$ is upper bounded due to boundness of $\{\mathcal{Y}_n^k\}, \forall n \in \mathbb{N}$. Then,

$$\sum_{n=1}^N \lambda_n \|V_n^k\|_* + \lambda \|\mathcal{E}^k\|_1 = \mathcal{L}_{\mu^k}(\mathcal{U}^k, \mathfrak{Y}^k, \mathcal{E}^k, \mathfrak{Y}^k) - \frac{1}{2\mu^{k-1}} \sum_{n=1}^N \left(\|\mathcal{Y}_n^k\| - \|\mathcal{Y}_n^{k-1}\| \right) \quad (\text{A.10})$$

is also upper bounded, which means that $\{V_n^k\}, \forall n \in \mathbb{N}$ and $\{\mathcal{E}^k\}$ are bounded. Since $\|U_n^k V_n^k\|_* = \|V_n^k\|_*$, $\{U_n^k V_n^k\}, \forall n \in \mathbb{N}$ are bounded as well. ■

B Proof of Theorem 4.1

Proof (I) The boundedness of $\mathcal{Y}_n^k, \hat{\mathcal{Y}}_n^k$ and $\bar{\mathcal{Y}}_n^k$ and the fact $\lim_{k \rightarrow \infty} \mu^k \rightarrow \infty$ imply that

$$\frac{\mathcal{Y}_n^{k+1} - \mathcal{Y}_n^k}{\mu^k} \rightarrow 0, \quad \frac{\hat{\mathcal{Y}}_n^{k+1} - \hat{\mathcal{Y}}_n^k}{\mu^k} \rightarrow 0, \quad \frac{\bar{\mathcal{Y}}_n^{k+1} - \bar{\mathcal{Y}}_n^k}{\mu^k} \rightarrow 0, \quad \forall n \in \mathbb{N}$$

By the definitions of $\{\mathcal{Y}_n^k\}, \{\hat{\mathcal{Y}}_n^k\}$ and $\{\bar{\mathcal{Y}}_n^k\}$, we have that

$$\begin{aligned} \mathcal{E}^{k+1} - \mathcal{E}^k &= \frac{\hat{\mathcal{Y}}_n^{k+1} - \mathcal{Y}_n^{k+1}}{\mu^k}, \quad \forall n \in \mathbb{N}, \\ V_n^{k+1} - V_n^k &= \frac{(U_n^{k+1})^T \left(\bar{\mathcal{Y}}_{n,(n)}^{k+1} - \hat{\mathcal{Y}}_{n,(n)}^{k+1} \right)}{\mu^k}, \quad \forall n \in \mathbb{N}, \\ U_n^{k+1} V_n^{k+1} - U_n^k V_n^k &= \frac{(1 + \rho) \mathcal{Y}_{n,(n)}^k - \left(\hat{\mathcal{Y}}_n^{k+1} + \rho \mathcal{Y}_{n,(n)}^{k+1} \right)}{\mu^k}, \quad \forall n \in \mathbb{N}. \end{aligned}$$

Therefore, the sequences $\{V_n^k\}, \{U_n^k V_n^k\}, \forall n \in \mathbb{N}$ and $\{\mathcal{E}^k\}$ are Cauchy sequences.

(II) It is easy to check that

$$\mathcal{T} - \text{fold}_n(U_n^{k+1} V_n^{k+1}) - \mathcal{E}^{k+1} = \frac{\mathcal{Y}_n^{k+1} - \mathcal{Y}_n^k}{\mu^k}. \quad (\text{B.1})$$

By the boundness of $\{\mathcal{Y}_n^k\}, \forall n \in \mathbb{N}$ and $\lim_{k \rightarrow \infty} \mu^k \rightarrow \infty$, we have that

$$\lim_{k \rightarrow \infty} \mathcal{T} - \text{fold}_n(U_n^{k+1} V_n^{k+1}) - \mathcal{E}^{k+1} \rightarrow 0, \quad (\text{B.2})$$

and thus $(U_n^k, V_n^k, \mathcal{E}^k), \forall n \in \mathbb{N}$ approaches to a feasible solution. ■

C Proof of Lemma 2

To prove Lemma 2, we need to introduce the following lemma.

Lemma C.1 [17] *Let X , Y and Q be matrices of compatible dimensions. If Q obeys $Q^T Q = I$ and $Y \in \partial \|X\|_*$, then $QY \in \partial \|X\|_*$.*

Proof of Lemma 2 Let the skinny SVD of G_n^k be $G_n^k = \hat{U}_n^k \hat{\Sigma}_n^k (\hat{V}_n^k)^T$, then it can be computed that

$$U_n^{k+1} = \hat{U}_n^k (\hat{V}_n^k)^T (V_n^k)^T.$$

Let the full SVD of $\hat{\Sigma}_n^k (\hat{V}_n^k)^T (V_n^k)^T$ be $\hat{\Sigma}_n^k (\hat{V}_n^k)^T (V_n^k)^T = \tilde{U}_n^k \tilde{\Sigma}_n^k (\tilde{V}_n^k)^T$. Note that \tilde{U}_n^k and \tilde{V}_n^k are orthogonal matrices, then we have that

$$U_n^{k+1} = \hat{U}_n^k \tilde{U}_n^k (\tilde{V}_n^k)^T,$$

which simply implies that

$$U_n^{k+1} (U_n^{k+1})^T = \hat{U}_n^k \tilde{U}_n^k (\tilde{V}_n^k)^T \tilde{V}_n^k (\tilde{U}_n^k)^T (\hat{U}_n^k)^T = \hat{U}_n^k (\hat{U}_n^k)^T.$$

Hence,

$$\begin{aligned} \hat{\mathcal{Y}}_{n,(n)}^{k+1} &= \mu^k \left(\left(\mathcal{T}_{(n)} - \mathcal{E}_{(n)}^k + \frac{\mathcal{Y}_{n,(n)}^k}{\mu^k} \right) - U_n^{k+1} (U_n^{k+1})^T \left(\mathcal{T}_{(n)} - \mathcal{E}_{(n)}^k + \frac{\mathcal{Y}_{n,(n)}^k}{\mu^k} \right) \right) \\ &= \mu^k (\hat{U}_n^k \hat{\Sigma}_n^k (\hat{V}_n^k)^T - U_n^{k+1} (U_n^{k+1})^T \hat{U}_n^k \hat{\Sigma}_n^k (\hat{V}_n^k)^T) \\ &= \mu^k (\hat{U}_n^k \hat{\Sigma}_n^k (\hat{V}_n^k)^T - \hat{U}_n^k (\hat{U}_n^k)^T \hat{U}_n^k \hat{\Sigma}_n^k (\hat{V}_n^k)^T) \\ &= \mu^k (\hat{U}_n^k \hat{\Sigma}_n^k (\hat{V}_n^k)^T - \hat{U}_n^k \hat{\Sigma}_n^k (\hat{V}_n^k)^T) = 0, \end{aligned}$$

i.e.,

$$\hat{\mathcal{Y}}_{n,(n)}^{k+1} = U_n^{k+1} (U_n^{k+1})^T \hat{\mathcal{Y}}_{n,(n)}^{k+1}. \quad (\text{C.1})$$

According to (A.7) and Lemma C.1, we have

$$U_n^{k+1} (U_n^{k+1})^T \hat{\mathcal{Y}}_{n,(n)}^{k+1} \in \lambda_n \partial \|U_n^{k+1} V_n^{k+1}\|_*, \quad \text{and thus } \hat{\mathcal{Y}}_{n,(n)}^{k+1} \in \lambda_n \partial \|U_n^{k+1} V_n^{k+1}\|_*. \quad (\text{C.2})$$

Since (A.5) and (C.2) hold for any k , they naturally hold at $(\{U^*\}, \{V^*\}, \mathcal{E}^*)$

$$\hat{\mathcal{Y}}_{n,(n)}^* \in \lambda_n \|U_n^* V_n^*\|_*, \quad \sum_{n=1}^N \mathcal{Y}_n^* \in \partial \|\mathcal{E}^*\|_1. \quad (\text{C.3})$$

Given any feasible solution $(\{U_n\}, \{V_n\}, \mathcal{E})$ to problem (3), by the convexity of nuclear norm and ℓ_1 norm, we have that

$$\begin{aligned} \sum_{n=1}^N \lambda_n \|V_n\|_* + \|\mathcal{E}\|_1 &= \sum_{n=1}^N \lambda_n \|U_n V_n\|_* + \|\mathcal{E}\|_1 \\ &\geq \sum_{n=1}^N \left(\lambda_n \|U_n^* V_n^*\|_* + \langle \hat{\mathcal{Y}}_{n,(n)}^*, U_n V_n - U_n^* V_n^* \rangle \right) + \|\mathcal{E}^*\|_1 + \left\langle \sum_{n=1}^N \mathcal{Y}_n^*, \mathcal{E} - \mathcal{E}^* \right\rangle \\ &= \sum_{n=1}^N \lambda_n \|U_n^* V_n^*\|_* + \|\mathcal{E}^*\|_1 + \sum_{n=1}^N \langle \mathcal{Y}_n^* - \hat{\mathcal{Y}}_{n,(n)}^*, \mathcal{E} - \mathcal{E}^* \rangle + \sum_{n=1}^N \langle \hat{\mathcal{Y}}_{n,(n)}^*, \text{fold}_n(U_n V_n) + \mathcal{E} - \text{fold}_n(U_n^* V_n^*) - \mathcal{E}^* \rangle \end{aligned}$$

By Theorem 1, we have that

$$\|\text{fold}_n(U_n V_n) + \mathcal{E} - \text{fold}_n(U_n^* V_n^*) - \mathcal{E}^*\|_\infty \leq \|\mathcal{T} - \text{fold}_n(U_n^* V_n^*) - \mathcal{E}^*\|_\infty \leq \varepsilon,$$

which directly leads to

$$\begin{aligned} & |\langle \hat{\mathcal{Y}}_n^*, \text{fold}_n(U_n V_n) + \mathcal{E} - \text{fold}_n(U_n^* V_n^*) - \mathcal{E}^* \rangle| \\ & \leq \|\hat{\mathcal{Y}}_n^*\|_\infty \|\text{fold}_n(U_n V_n) + \mathcal{E} - \text{fold}_n(U_n^* V_n^*) - \mathcal{E}^*\|_1 \\ & = \|\hat{\mathcal{Y}}_{n,(n)}^*\|_\infty \|\text{fold}_n(U_n V_n) + \mathcal{E} - \text{fold}_n(U_n^* V_n^*) - \mathcal{E}^*\|_1 \\ & \leq \|\hat{\mathcal{Y}}_{n,(n)}^*\| \|\text{fold}_n(U_n V_n) + \mathcal{E} - \text{fold}_n(U_n^* V_n^*) - \mathcal{E}^*\|_\infty \\ & \leq \lambda_n I_n \prod_{m \neq n} I_m \varepsilon \end{aligned}$$

where $\|\hat{\mathcal{Y}}_{n,(n)}^*\| \leq \lambda_n$ is due to (C.3). Hence, we complete the proof. \blacksquare

D Proof of Theorem 2

Proof Note that $(\{U_n\} = \mathbf{0}, \{V_n\} = \mathbf{0}, \mathcal{E} = \mathcal{T})$ is feasible to (3) and let $(\{U_n^g\}, \{V_n^g\}, \mathcal{E}^g)$ be a globally optimal solution to (3), then we have

$$\|\mathcal{E}^g\|_1 \leq \sum_{n=1}^N \lambda_n \|V_n^g\|_* + \|\mathcal{E}^g\|_1 \leq \|\mathcal{T}\|_1.$$

By the proof of Lemma 1, we have that $\mathcal{Y}_n^* = \mathcal{Y}_m^*, \forall n, m \in \mathbb{N}, n \neq m$ almost surely since $\mathcal{Y}_n^0 = \mathcal{Y}_m^0 = \mathbf{0}$. Recall that $\|\sum_{n=1}^N \mathcal{Y}_n^{k*}\|_\infty \leq 1$, and we have that $\|\mathcal{Y}_n^{k*}\|_\infty \leq \frac{1}{N}, \forall n \in \mathbb{N}$. So

$$\|\mathcal{Y}_n^{k*}\|_F = \|\mathcal{Y}_{n,(n)}^{k*}\|_F \leq \sqrt{I_n \prod_{m \neq n} I_m} \|\mathcal{Y}_{n,(n)}^{k*}\|_\infty = \sqrt{I_n \prod_{m \neq n} I_m} \|\mathcal{Y}_n^{k*}\|_\infty \leq \sqrt{I_n \prod_{m \neq n} I_m} \frac{1}{N}$$

holds and thus \mathcal{E}^* is bounded by

$$\begin{aligned} \|\mathcal{E}^*\|_1 & \leq \sum_{n=1}^N \lambda_n \|V_n^*\|_* + \|\mathcal{E}^*\|_1 \\ & \leq \mathcal{L}_{\mu^{k^*}}(\mathfrak{U}^{k^*+1}, \mathfrak{V}^{k^*+1}, \mathcal{E}^{k^*+1}, \mathfrak{Y}^{k^*+1}) + \sum_{n=1}^N \frac{\|\mathcal{Y}_n^{k^*}\|_F^2}{2\mu^{k^*}} \\ & \leq \sum_{n=1}^N \frac{1}{\mu^0 N^2} I_n \prod_{m \neq n} I_m \left(\frac{\rho(1+\rho)}{\rho-1} + \frac{1}{2\rho^{k^*}} \right). \end{aligned} \tag{D.1}$$

Hence, $\|\mathcal{E}^g - \mathcal{E}^*\|_1 \leq \|\mathcal{E}^g\|_1 + \|\mathcal{E}^*\|_1 \leq c$. By Lemma 2, we have

$$\begin{aligned}
f^g &= \sum_{n=1}^N \lambda_n \|V_n^g\|_* + \|\mathcal{E}^g\|_1 \geq \sum_{n=1}^N \lambda_n \|V_n^*\|_* + \|\mathcal{E}\|_1 + \sum_{n=1}^N \langle \mathcal{Y}_n^* - \hat{\mathcal{Y}}_n^*, \mathcal{E}^g - \mathcal{E}^* \rangle \\
&\geq f^* - \left\| \sum_{n=1}^N \mathcal{Y}_n^* - \sum_{n=1}^N \hat{\mathcal{Y}}_n^* \right\|_\infty \|\mathcal{E}^g - \mathcal{E}^*\|_1 - \sum_{n=1}^N \lambda_n I_n \prod_{m \neq n} I_m \varepsilon \\
&\geq f^* - c\varepsilon - \sum_{n=1}^N \lambda_n I_n \prod_{m \neq n} I_m \varepsilon
\end{aligned}$$

which complete the proof. ■

E Proof of Theorem 3

Proof By the convexity of problem (1) and the optimality of $(\mathcal{X}^0, \mathcal{E}^0)$, it naturally follows that $f^0 \leq f^*$. Let $\mathcal{X}_{(n)}^0 = U_n^0 \Sigma_n^0 (V_n^0)^T$ be the skinny SVD of mode- n unfolding $\mathcal{X}_{(n)}^0$. Constructing $U'_n = U_n^0$, $V'_n = \Sigma_n^0 (V_n^0)^T$ and $\mathcal{E}' = \mathcal{E}^0$, we have the following equality when $R_n \geq r_n$,

$$\mathcal{T} = \mathcal{X}^0 + \mathcal{E}^0 = \text{fold}_n(U_n^0 \Sigma_n^0 (V_n^0)^T) + \mathcal{E}^0 = \text{fold}_n(U'_n V'_n) + \mathcal{E}' \quad (\text{E.1})$$

i.e., $(\{U'_n\}, \{V'_n\}, \mathcal{E}')$ is a feasible solution to problem (3). By Theorem 2, we can conclude that

$$f^* - c\varepsilon - \sum_{n=1}^N \lambda_n I_n \prod_{m \neq n} I_m \leq f^0.$$

For $R_n < r_n$, we decompose the skinny SVD of $\mathcal{X}_{(n)}^0$ as

$$\mathcal{X}_{(n)}^0 = U_n^1 \Sigma_n^1 (V_n^1)^T + U_n^2 \Sigma_n^2 (V_n^2)^T,$$

where U_n^1 and V_n^1 (resp. U_n^2 and V_n^2) are the singular vectors associated with the R_n largest singular values (resp. the rest singular values smaller than or equal to $\sigma_{(n)}^{R_n}$). With these notations, we have a feasible solution to problem (3) by constructing

$$U''_n = U_n^1, \quad V''_n = \Sigma_n^1 (V_n^1)^T, \quad \mathcal{E}'' = \mathcal{E}^0 + \text{fold}_n(U_n^2 \Sigma_n^2 (V_n^2)^T).$$

By Theorem 2, we have that

$$\begin{aligned}
f^* - c\epsilon - \sum_{n=1}^N \lambda_n I_n \prod_{m \neq n} I_m &\leq f^g \leq \sum_{n=1}^N \|V_n''\|_*^2 + \|\mathcal{E}''\|_1 \\
&= \sum_{n=1}^N \lambda_n \left(\|\Sigma_n^1 (V_n^1)^T\|_* + \|\mathcal{E}^0 + \text{fold}_n(U_n^2 \Sigma_n^2 (V_n^2)^T)\|_1 \right) \\
&\leq \sum_{n=1}^N \lambda_n \left(\|\mathcal{X}_{(n)}^0\|_* - \|\Sigma_n^2\|_* + \|\mathcal{E}^0 + \text{fold}_n(U_n^2 \Sigma_n^2 (V_n^2)^T)\|_1 \right) \\
&\leq f^0 + \sum_{n=1}^N \lambda_n \left(\|U_n^2 \Sigma_n^2 (V_n^2)^T\|_1 - \|\Sigma_n^2\|_* \right) \\
&\leq f^0 + \sum_{n=1}^N \lambda_n \left(\sqrt{I_n \prod_{m \neq n} I_m} \|U_n^2 \Sigma_n^2 (V_n^2)^T\|_* - \|\Sigma_n^2\|_* \right) \\
&= f^0 + \sum_{n=1}^N \lambda_n \left(\sqrt{I_n \prod_{m \neq n} I_m} - 1 \right) \|\Sigma_n^2\|_* \\
&\leq f^0 + \sum_{n=1}^N \lambda_n \left(\sqrt{I_n \prod_{m \neq n} I_m} - 1 \right) \sigma_{(n)}^{R_n+1} (r_n - R_n),
\end{aligned}$$

which complete the proof. ■